



Radioactive and  
radiogenic isotopes in  
Ngarradj (Swift Creek)  
sediments: a baseline  
study

---

A Bollhöfer & P Martin

February 2003

# Radioactive and radiogenic isotopes in Ngarradj (Swift Creek) sediments: a baseline study

A Bollhöfer & P Martin

Environmental Research Institute of the Supervising Scientist  
Supervising Scientist Division  
Environment Australia



# Contents

<b>1 Introduction</b>	<b>1</b>
<b>2 Methods</b>	<b>4</b>
2.1 Sample collection	4
2.2 Gamma Spectrometry	4
2.3 Inductively Coupled Plasma Mass Spectrometry (ICPMS)	5
2.4 Pb isotope systematics	7
<b>3 Results</b>	<b>8</b>
3.1 Uranium series elements	8
3.2 Thorium series elements and potassium	8
3.3 Chemistry	11
<b>4 Discussion</b>	<b>17</b>
4.1 Characterization of Ngarradj sediments in comparison to other sediments within the Alligator Rivers Region	17
4.2 Radiogenic and Radioactive Isotopes	18
<b>Acknowledgements</b>	<b>21</b>
<b>References</b>	<b>21</b>
<b>Figures</b>	
Figure 1 The Ngarradj (Swift Creek) catchment and tributaries showing the Jabiluka mine lease and the approximate mine location	2
Figure 2 Stability checks for detector O during the time period measured	5
Figure 3 Results of the measurements of certified standard material 2704 and MESS-2 via ICP-MS at Northern Territory University, Darwin	6
Figure 4 Pb isotope systematics	7
Figure 5 Comparison of <sup>40</sup> K data measured via gamma spectrometry at eriss and ICPMS and NTU	11
Figure 6 Copper, zinc and manganese concentration measured by ICP-MS in sediments of the Ngarradj catchment	11

Figure 7 Magnesium, aluminium, iron and potassium concentration measured by ICP-MS in sediments of the Ngarradj catchment	13
Figure 8 Pb isotope ratios of Ngarradj sediments in comparison with isotope ratios measured in aerosols worldwide	14
Figure 9 $^{206}\text{Pb}/^{207}\text{Pb}$ isotope ratios in sediments from Ngarradj. Pb isotope ratios are higher, i.e. more radiogenic for sediments from the control sites	14
Figure 10 $^{208}\text{Pb}/^{207}\text{Pb}$ isotope ratios in sediments from Ngarradj. Pb isotope ratios are higher, i.e. more radiogenic for sediments from the control sites.	15
Figure 11 $^{226}\text{Ra}$ versus $^{228}\text{Ra}$ activity concentration	15
Figure 12 Ra isotope ratios in the different tributaries in the Ngarradj catchment	16
Figure 13 Inverse $^{226}\text{Ra}$ concentration plot. Uncertainties are one standard deviation of counting statistics.	16
Figure 14 $^{208}\text{Pb}/^{206}\text{Pb}$ isotope ratios plotted versus thorium activity concentration	18
Figure 15 Inverse Pb concentration plots identifying the source of contaminant Pb	20

## Tables

Table 1 Samples taken for gamma analysis. Asterisks indicate the samples that were analysed via ICP-MS for trace metals and Pb isotopes	3
Table 2 Uranium series elements (Bq/kg) in Ngarradj catchment sediments	9
Table 3 Thorium series elements and K-40 in Ngarradj catchment sediments	10
Table 4 ICP-MS results for heavy metals, Mg, K, U and Pb in ppm and Pb isotope ratios.	12
Table 5 Averages (or ranges) of $^{238}\text{U}$ , $^{232}\text{Th}$ and $^{40}\text{K}$ activity concentrations in sediments of the Alligator Rivers Region	17

# Radioactive and radiogenic isotopes in Ngarradj (Swift Creek) sediments: a baseline study

A Bollhöfer & P Martin

## 1 Introduction

In 1977, the Australian Government authorised the mining and export of uranium in the Alligator Rivers Region. This included the mining leases at Ranger, approved in 1977, Jabiluka, approved in 1998, and Koongarra. The environmental protection plan for the mining leases had three essential elements:

- the granting of land to Traditional Owners,
- the establishment of Kakadu National Park and
- the establishment of a Supervising Scientist.

After the implementation of the Environmental Protection Plan, mining and milling of uranium at the open-cut Ranger Mine commenced in 1981 and will probably be completed by 2007 (Johnston and Prendergast, 1999). Decline and underground works at the underground mine Jabiluka commenced in 1998 and the first stage of the development was finished in 1999. Currently, the Jabiluka Project is on a standby modus.

There are two alternatives for the milling of the Jabiluka uranium ore. One possibility is to mine and mill the ore on the Jabiluka mine site. This would involve the storage of waste rock and ore on the surface of the mine and 25 % of the tailings would be stored in a large tailings dam, whereas the other 75 % would be stored as cement paste in the voids of the mine. The second possibility is to transport the uranium ore via a haul road from Jabiluka to Ranger mine and use the existing milling facilities at Ranger to process the Jabiluka ore. ERA was proposing to mine and mill the ore at Jabiluka, which has been approved, based on all the tailings being eventually returned to the underground mine voids. Regardless which milling alternative is chosen, waste rock and ore stockpiles will be stored on the surface of the mine lease.

Approximately 90 % of the rainfall falling onto Jabiluka becomes runoff (Chiew and Wang, 1999). The legislative requirements are such that runoff, erosion products and surface water that was in contact with the stockpiles will have to be contained in the retention pond and are not meant to leave the Total Containment Zone (TCZ). Whereas surface waters from the Mine Valley, above Jabiluka ore body 2, drain towards the west into Magela floodplain, surface water on the eastern side of the topographic divide, including Jabiluka mine, drain into the Ngarradj (Swift Creek) catchment and finally into the Magela Creek floodplain several kilometres north of the ore body.

Fears have been expressed by Traditional Owners and environmental organisations that the development of the Jabiluka project might have an adverse effect on Kakadu National Park, although Rio Tinto, who now own Energy Resources Australia (ERA), have announced a 10 year moratorium on the mining of Jabiluka (an announcement made at the company's Annual General Meeting on April 12, 2001, in London). However, the Jabiluka lease, with an area of 73 km<sup>2</sup> at the edge of Kakadu National Park, might be sold by Rio Tinto or economic developments might make the mining of uranium at Jabiluka more profitable. Therefore, a baseline dataset is needed to be able to assess impacts of mining of uranium at the Jabiluka mine should this occur.

Baseline studies investigating radionuclide and heavy metal concentrations in surface waters and biota have previously been conducted. The present study aims to produce a baseline dataset for sediments of the Ngarradj catchment to be able to estimate a possible impact of erosion from the Jabiluka mine site on the composition of sediments of the Ngarradj catchment. The current report focuses on a chemical and radiochemical dataset relevant to sediments from the Ngarradj catchment.

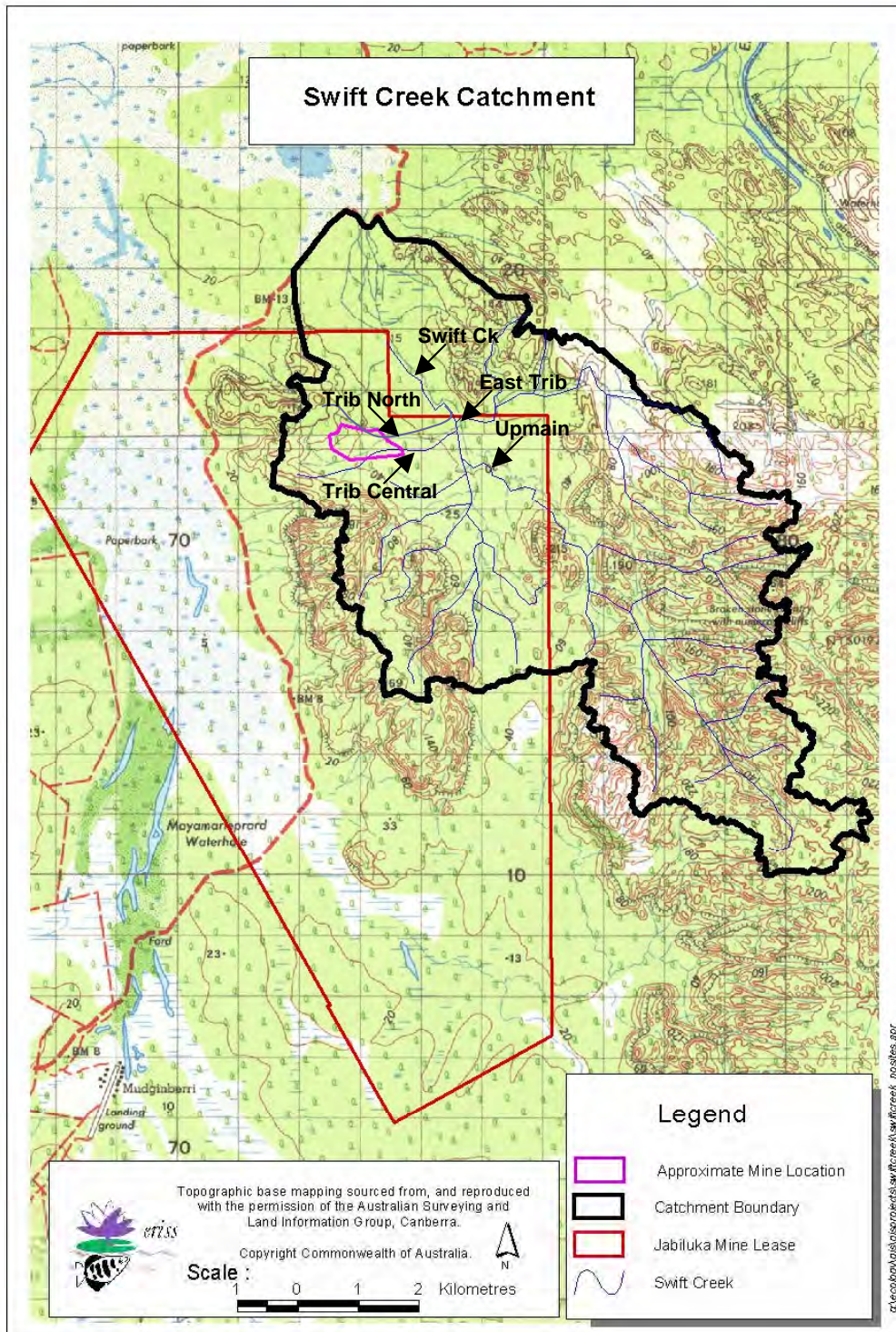


**Figure 1** The Ngarradj (Swift Creek) catchment and tributaries showing the Jabiluka mine lease and the approximate mine location

**Table 1** Samples taken for gamma analysis. Asterisks indicate the samples that were analysed via ICP-MS for trace metals and Pb isotopes

<b>Cast Code</b>	<b>name EnRad</b>	<b>Sample Name HEP</b>	<b>Description</b>	<b>Date</b>
JB334	SW0126	Swift Creek TC07C	Tributary Central, cross section 07C	2/10/01
JB335	SW0127*	Swift Creek TC03	Tributary Central, cross section 03	2/10/01
JB336	SW0128*	Swift Creek TC06C	Tributary Central, cross section 06C	2/10/01
JB337	SW0129*	Swift Creek TC04	Tributary Central, cross section 04	2/10/01
JB338	SW0130*	Swift Creek TC05	Tributary Central, cross section 05	2/10/01
JB339	SW0131*	Swift Creek TN01	Tributary North, cross section 01	2/10/01
JB340	SW0132	Swift Creek TN03	Tributary North, cross section 03	2/10/01
JB341	SW0133	Swift Creek TN02	Tributary North, cross section 02	2/10/01
JB342	SW0134*	Swift Creek TN04	Tributary North, cross section 04	2/10/01
JB343	SW0135	Swift Creek TN07	Tributary North, cross section 07	2/10/01
JB344	SW0136	Swift Creek TN08	Tributary North, cross section 08	2/10/01
JB345	SW0137*	Swift Creek TN09	Tributary North, cross section 09	2/10/01
JB350	SW0142*	Swift Creek UM01	Upmain, cross section 01	2/10/01
JB351	SW0143	Swift Creek UM02	Upmain, cross section 02	2/10/01
JB352	SW0144	Swift Creek UM04	Upmain, cross section 04	2/10/01
JB353	SW0145*	Swift Creek UM06	Upmain, cross section 06	2/10/01
JB354	SW0146*	Swift Creek ET01	East Tributary, cross section 01	2/10/01
JB355	SW0147	Swift Creek ET03	East Tributary, cross section 03	2/10/01
JB356	SW0148	Swift Creek ET04	East Tributary, cross section 04	2/10/01
JB357	SW0149	Swift Creek ET06	East Tributary, cross section 06	2/10/01
JB360	SW0152	Swift Creek ET07	East Trib Cross Section 07	2/10/01
JB358	SW0150*	Swift Creek ET08	East Trib Cross Section 08	2/10/01
JB359	SW0151	Swift Creek SM01	Swift Creek, cross section 01	2/10/01
JB349	SW0141	Swift Creek SM03	Swift Creek, cross section 03	2/10/01
JB347	SW0139	Swift Creek SM04	Swift Creek, cross section 04	2/10/01
JB348	SW0140*	Swift Creek SM05	Swift Creek, cross section 05	2/10/01
JB346	SW0138*	Swift Creek SM08	Swift Creek, cross section 08	2/10/01
N/A	SW02009*	Swift Creek SM08	Swift Creek, cross section 08	30/5/02
N/A	SW02010*	Swift Creek ET08	East Trib Cross Section 08	30/5/02
N/A	SW02011*	Swift Creek TN01	Tributary North, cross section 01	30/5/02
N/A	SW02012*	Swift Creek TC05	Tributary Central, cross section 05	30/5/02

Both the Ngarradj Central Tributary and Tributary North flow through the lease and might be potentially affected by mining activities (figure 1). These two mine site tributaries will be investigated in more detail. Other tributaries include the East Tributary and the Upper Main Ngarradj, which have not been in contact with the mine lease at all. These two tributaries will be regarded as control sites.

The sampling regime focuses on the collection of samples at the end of each dry season and will be continued for several years to obtain a statistically relevant dataset.

This first report presents and discusses the data and peculiarities of the first year of sampling. Table 1 gives a description of the samples taken in October 2001. Asterisks mark those samples that have been analysed using ICP-MS for major chemical constituents, heavy metals and Pb isotopes. Four additional samples were taken May 30, 2002, for ICP-MS analysis.

## 2 Methods

### 2.1 Sample collection

Scrape samples were collected from various cross sections along 4 tributaries of Ngarradj, and in addition from the main channel in early October 2001, by the Hydrological and Ecological Processes (*HEP*) section of *eriss*. Two tributaries, the East Tributary and Upmain Swift, are regarded as background or control sites and will largely be unaffected by activities at Jabiluka, whereas the North and Central Tributaries are passing the mine lease and could possibly be influenced by run-off, irrigation water or erosion from the mine site (figure 1).

Samples were dried, sieved and the fraction < 2mm was ground in a *Labtechnics* milling machine. A fraction of the sample was taken for heavy metal and lead isotope analysis via ICP-MS. For gamma spectrometry, approximately 16 g of the sediment were cast with an epoxy resin and counted for a period of 1 – 2 days.

Additional samples were taken in June 2002 to double-check for possible contamination effects that might have occurred during sieving and milling of the earlier samples. Samples were collected using plastic polyethylene (PET) gloves and acid-cleaned plastic bags and approximately 1 cm of the top sediment were removed. No further sample preparation was conducted and samples were sent to Northern Territory University (NTU), Darwin, for analysis via ICP-MS.

### 2.2 Gamma Spectrometry

$^{238}\text{U}$ ,  $^{226}\text{Ra}$ ,  $^{228}\text{Ra}$ ,  $^{228}\text{Th}$ ,  $^{210}\text{Pb}$  and  $^{40}\text{K}$  activities in the sediments were determined using the High Purity Germanium (HPGe) gamma detectors from the Environmental Radioactivity section at *eriss*. Procedures for sample collection, preparation and measurements of radionuclide activity concentrations via gamma spectroscopy at the Environmental Radioactivity laboratory are described in Marten (1986).

Results given in the results file contain the radionuclide activity concentrations of the long-lived progeny of uranium series, thorium series and miscellaneous other photo peaks, such as  $^{40}\text{K}$ ,  $^{137}\text{Cs}$  and  $^7\text{Be}$ . The stability of the detectors is checked fortnightly with a multi isotope standard containing radionuclides of the uranium and thorium decay chains. The results of the stability checks over the period when the Ngarradj samples were analysed are shown in figure 2. Due to a change in geometric efficiency, measurements of the stability check radionuclide concentrations gave results at approximately 4 per cent higher than the long term average. Therefore, Ngarradj sediment radionuclide concentrations have been corrected accordingly.

Detection limits for the geometry used are approximately 15 Bq/kg for  $^{238}\text{U}$  and  $^{210}\text{Pb}$  and approximately 3.5 Bq/kg for  $^{226}\text{Ra}$ ,  $^{228}\text{Ra}$  and  $^{228}\text{Th}$  (Marten, 1986).

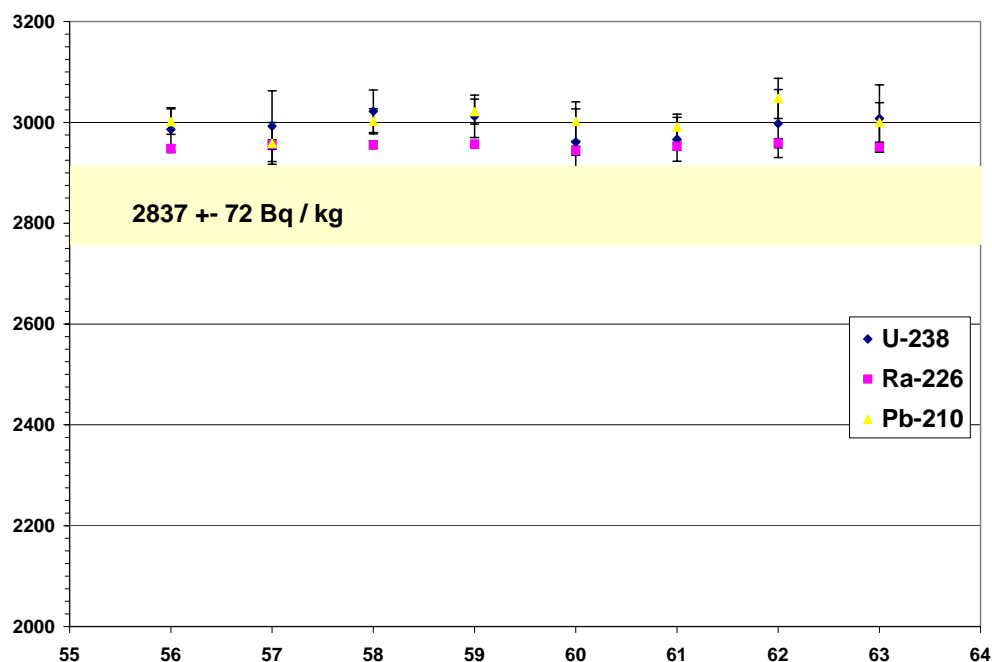


**Figure 2** Stability checks for detector O during the time period measured. Uncertainties are one standard deviation due to counting statistics only. Stability checks were on average 4.5 % above the long-term average of  $2837 \pm 70$  (1 s.d.) for both members of the U and Th series, due to a change in geometric detection efficiency of the detector. Data from Ngarradj sediments have been corrected accordingly.

### 2.3 Inductively Coupled Plasma Mass Spectrometry (ICPMS)

Pb isotopes and trace metal contents of the sediments have been analysed by ICP-MS at Northern Territory University, Darwin.

Samples were digested in a nitric/perchloric acid mixture. An aliquot was taken for ICP-MS, dried down and re-dissolved in 10% nitric acid, before the sample was injected into the plasma torch of the *Perkin Elmer Elan 6000 ICP-MS*. Details of the operating system and sample preparation technique can be found in Munksgaard et al. (1998) and Munksgaard and Parry (2000). Typical uncertainties for the Pb isotope ratios are 0.5 – 1 % relative standard deviation.

With every set of samples, 2704 and MESS-2 certified standard material was measured. Results of those measurements, and thus the accuracy of the ICP-MS measurements, are shown in figure 3. Apart from cadmium, levels reported were well above the detection limits. Whereas measurements of aluminium, potassium and calcium via ICP-MS at NTU were generally lower than certified values (figure 3a), results for heavy metals, Fe and minor chemical constituents agree well with the certified values within uncertainties (figure 3 b).

To check for possible contamination of the samples, four additional sediment samples were taken in May 2002. These samples were neither sieved nor milled, to avoid contaminating the samples with matter from earlier sieving and milling activities. Ultra-clean procedures were used during collection. After sending the samples to NTU the samples were dried, digested in

a nitric/perchloric acid mixture, dried down and re-dissolved in 10% nitric acid prior to the ICP-MS measurements.

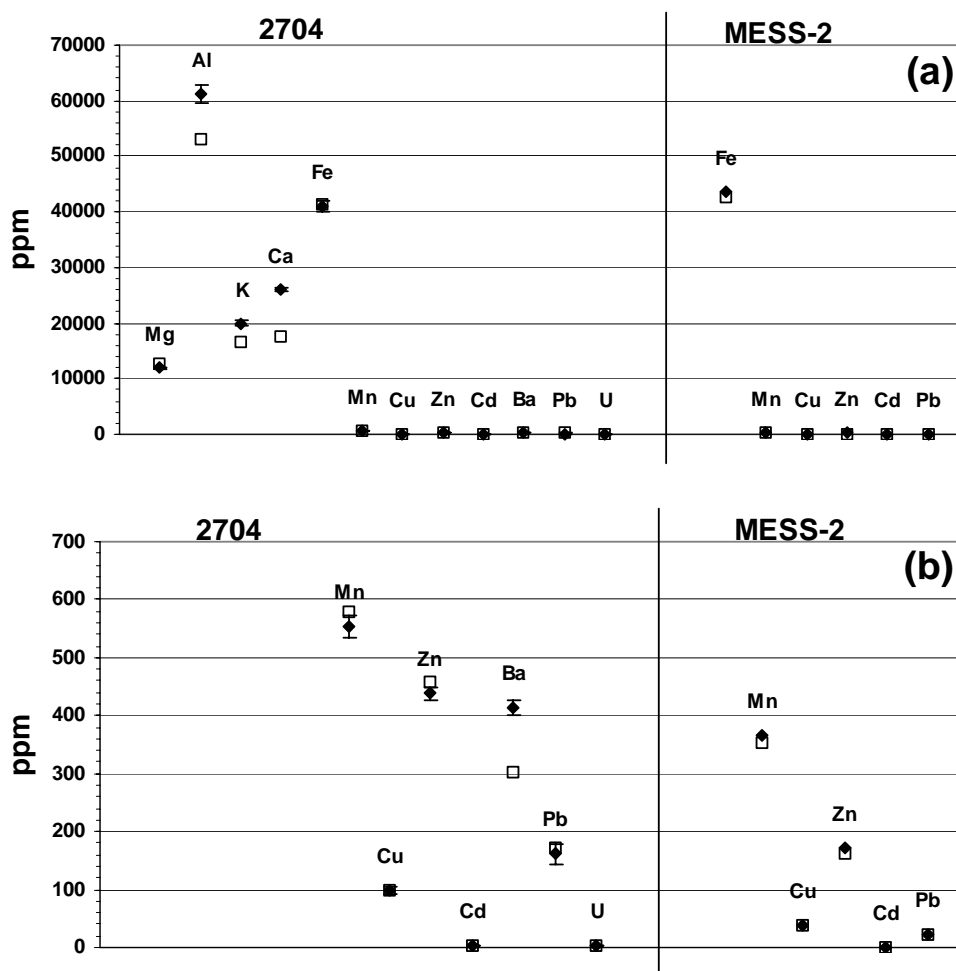


**Figure 3** Results of the measurements of certified standard material 2704 and MESS-2 via ICP-MS at Northern Territory University, Darwin. Uncertainties reported are 2 s.d.

It is important to note that the element concentration in sediments determined via ICP-MS (and other techniques utilizing a chemical digestion method) may strongly depend on the digestion technique used and the sample mineral composition. This has been shown for rare earth elements (Munksgaard and Parry, in prep.) and also applies to some actinides. For example,  $U^{4+}$  may enter the zircon structure because, like  $Zr^{4+}$ , it has a large ionic radius. The uranium, bound in the mineral lattice of the zircon, will be difficult to dissolve and therefore digestion techniques, in contrast to gamma spectrometry, may underestimate the actual uranium concentration in the sample. This is especially the case for samples with a high proportion of sands, quartzes, heavy minerals etc., and a low proportion of silts and clays. Samples studied from the Ngarradj catchment had sand contents of 90-99 per cent.

Contamination of low concentration samples with radiogenic Pb can have a drastic effect on the Pb isotope ratios, as they can differ by orders of magnitude. For instance, Bollhöfer and Rosman (2000, 2001) report a range of  $^{208}Pb/^{206}Pb$  ( $^{207}Pb/^{206}Pb$ ) ratios for aerosols collected worldwide of 2.006-2.204 (0.812-0.943). Gulson et al. (1992) report a background  $^{208}Pb/^{206}Pb$  ratio of 2.1764 for the Alligator Rivers region. However,  $^{208}Pb/^{206}Pb$  ( $^{207}Pb/^{206}Pb$ ) isotope ratios, for example in particulates from tailings dam surface waters, can

be as low as 0.0051 (0.1032) (Gulson et al., 1992). Hence the contamination of a background dust sample with for instance 5 % of its Pb originating from dried tailings will shift the  $^{208}\text{Pb}/^{206}\text{Pb}$  isotope ratios in background samples from 2.1764 to 2.0678. Similarly, minerals with high  $^{208}\text{Pb}/^{206}\text{Pb}$  isotope ratios will shift the ratios of the composite sample towards higher values.

## 2.4 Pb isotope systematics

Measurements of Pb isotope ratios have been applied extensively in environmental studies and to identify anthropogenic pollution. They have mainly been used to distinguish and trace origin of pollution via the different sources of Pb in leaded petrol (Chow et al., 1975; Rosman et al., 1993; Bollhöfer and Rosman, 2000, 2001). However, there are more environmental applications, as shown for example by Rosman et al. (1997) or Munksgaard and Parry (2000). Particular in U mining, Pb isotopes provide a powerful and sensitive tool to identify mine derived contaminants both, air- and waterborne. This is due to the comparably high amount of radiogenic Pb in mine derived material.

Whereas primordial (or common) Pb is Pb that has existed since the beginning of the earth at a fixed relative isotope abundance, the radiogenic Pb is produced by the radioactive decay of  $^{238}\text{U}$ ,  $^{235}\text{U}$  and  $^{232}\text{Th}$  (figure 4). The Pb isotopes  $^{206}\text{Pb}$ ,  $^{207}\text{Pb}$  and  $^{208}\text{Pb}$  are the endmembers of the uranium and thorium decay chains, whereas  $^{204}\text{Pb}$  is the only exclusively primordial isotope. Therefore, different minerals for example, will exhibit different  $^{206}\text{Pb}/^{204}\text{Pb}$ ,  $^{207}\text{Pb}/^{204}\text{Pb}$  and  $^{208}\text{Pb}/^{204}\text{Pb}$  isotope ratios, dependent on the age and their initial uranium and thorium content. Consequently,  $^{206}\text{Pb}/^{207}\text{Pb}$  and  $^{208}\text{Pb}/^{207}\text{Pb}$  ratios will vary as well.

Due to different half-lives and the natural isotope ratio of  $^{238}\text{U}$  and  $^{235}\text{U}$  of 137.88, more radiogenic in general means higher  $^{206}\text{Pb}/^{207}\text{Pb}$  ratios. Dependent on the thorium content of the source rock, however,  $^{208}\text{Pb}/^{207}\text{Pb}$  ratios may either in- or decrease.

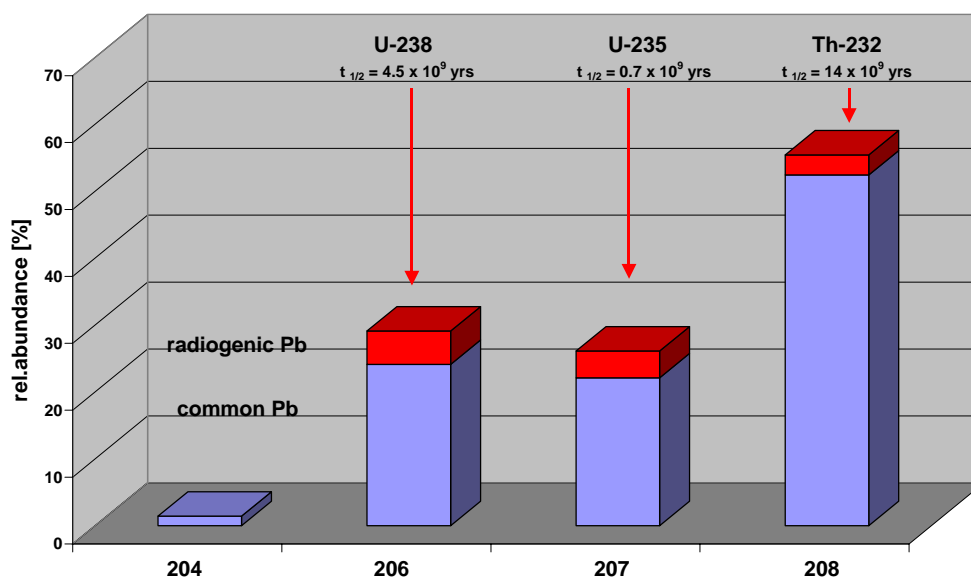


Figure 4 Pb isotope systematics

$^{206}\text{Pb}/^{207}\text{Pb}$  and  $^{208}\text{Pb}/^{207}\text{Pb}$  ratios in lead ores usually increase with decreasing age, i.e. the younger the lead ore body the more radiogenic Pb could be produced before its mineralization. In case of a uranium ore body, however, where highly concentrated uranium

decays to lead,  $^{206}\text{Pb}/^{207}\text{Pb}$  ratios are relatively more radiogenic, whereas  $^{208}\text{Pb}/^{207}\text{Pb}$  ratios are relatively low. For instance, Gulson et al. (1992) report ratios of 9.68 ( $^{206}\text{Pb}/^{207}\text{Pb}$ ) and 0.049 ( $^{208}\text{Pb}/^{207}\text{Pb}$ ) in particulates from surface waterbodies at Ranger mine.

$^{206}\text{Pb}/^{207}\text{Pb}$  isotope ratios in aerosols collected worldwide (Bollhöfer and Rosman, 2000, 2001) have been shown to vary between approximately 1.06, an isotope ratio typically found in relatively old Mt. Isa lead ore used to produce leaded petrol, up to 1.25 for relatively young Mississippi type Pb ores and modern Pb in dust (see also Munksgaard and Parry (2002)).  $^{206}\text{Pb}/^{207}\text{Pb}$  and  $^{208}\text{Pb}/^{207}\text{Pb}$  ratios in U/Th rich mineral grains, such as zircons, baddelytes or monazites, however, can be much higher.

## 3 Results

### 3.1 Uranium series elements

Table 2 shows the results of the gamma spectroscopic measurements of radionuclide activities for uranium series elements in Bq per kg.

Within 2 standard deviations the elements of the U decay series are in radioactive equilibrium, although some of the samples have an excess in  $^{210}\text{Pb}$ , in particular samples from Tributary North and Swift Main channel.

Activity concentration for uranium measured via gamma spectrometry are generally higher than the activity concentration calculated from the ICP-MS results. This is most likely due to the incomplete digestion of some of the uranium bearing minerals in the sample, whereas activity concentrations determined via gamma spectrometry are total sediment activities, independent of any chemical or physical digestion techniques used during sample preparation.

### 3.2 Thorium series elements and potassium

Table 3 shows the results of the gamma spectrometry measurements for thorium series elements and K-40 in Bq per kg. As for the uranium series, within 2 standard deviations, Ra and Th are in radioactive equilibrium. The variations in  $^{40}\text{K}$ -activities are quite large, due to the low potassium concentration in the sediments. However, activities in the Central Tributary appear to be on average higher as compared to the remaining tributaries.

Figure 5 shows a comparison of potassium data measured via gamma spectrometry and results from the ICP-MS measurements at NTU. Although samples were generally close to the detection limit for  $^{40}\text{K}$  using gamma spectrometry, the activity concentrations agree reasonable well within uncertainties.

**Table 2** Uranium series elements (Bq/kg) in Ngarradj catchment sediments. n.d.: below detection limit. Uncertainties are one standard deviation due to counting statistics only. TC: Tributary Central; TN: Tributary North; SM: Swift Main channel; UM: Upmain Ngarradj; ET: East Tributary.

<b>Eriss ID</b>	<b>Site</b>	<b>U-238</b>	<b>+ - abs</b>	<b>Ra-226</b>	<b>+ - abs</b>	<b>Pb-210</b>	<b>+ - abs</b>
SW0126	TC07c	29	4	24	1	25	5
SW0127	TC03	n.d.	n.d.	19	1	20	6
SW0128	TC06c	25	7	22	1	21	9
SW0129	TC04	16	7	12	1	13	7
SW0130	TC05	16	9	13	1	14	9
SW0131	TN01	34	8	28	1	41	10
SW0132	TN03	18	7	13	1	11	9
SW0133	TN02	18	7	6	1	7	8
SW0134	TN04	24	6	13	1	32	7
SW0135	TN07	19	5	10	1	18	6
SW0136	TN08	25	6	8	1	3	8
SW0137	TN09	19	4	20	1	31	5
SW0138	SM08	6	4	5	1	6	5
SW0139	SM04	7	4	5	1	10	5
SW0140	SM05	7	4	5	1	n.d.	n.d.
SW0141	SM03	11	4	7	1	18	6
SW0151	SM01	n.d.	n.d.	12	1	0	8
SW0142	UM01	11	4	8	1	9	5
SW0143	UM02	16	6	8	1	16	6
SW0144	UM04	n.d.	n.d.	9	1	15	7
SW0145	UM06	13	3	10	1	15	5
SW0146	ET01	12	6	9	1	15	9
SW0147	ET03	n.d.	n.d.	10	1	12	8
SW0148	ET04	16	6	15	1	15	8
SW0149	ET06	19	6	14	1	19	8
SW0150	ET08	18	10	11	1	0	8
SW0152	ET07	n.d.	n.d.	17	1	22	8

**Table 3** Thorium series elements and K-40 in Ngarradj catchment sediments. Uncertainties are one standard deviation of counting statistics only.

<b>Eriss ID</b>	<b>Site</b>	<b>Ra-228</b>	<b>+ - abs</b>	<b>Th-228</b>	<b>+ - abs</b>	<b>K-40</b>	<b>+ - abs</b>
SW0126	TC07c	24	1	23	1	8	5
SW0127	TC03	17	2	13	1	14	7
SW0128	TC06c	19	2	17	1	26	9
SW0129	TC04	12	2	15	1	16	8
SW0130	TC05	15	2	17	1	18	10
SW0131	TN01	31	3	26	1	29	10
SW0132	TN03	18	2	16	1	n.d.	n.d.
SW0133	TN02	13	2	13	1	14	9
SW0134	TN04	17	2	20	1	7	8
SW0135	TN07	15	1	16	1	2	6
SW0136	TN08	16	2	16	1	10	9
SW0137	TN09	20	1	20	1	8	5
SW0138	SM08	6	1	9	1	9	5
SW0139	SM04	8	1	8	1	11	5
SW0140	SM05	9	1	9	1	11	6
SW0141	SM03	10	1	8	1	14	6
SW0151	SM01	11	2	10	1	n.d.	n.d.
SW0142	UM01	10	1	8	1	11	5
SW0143	UM02	7	1	9	1	5	7
SW0144	UM04	11	2	8	1	6	7
SW0145	UM06	8	1	9	1	2	5
SW0146	ET01	9	2	13	1	15	9
SW0147	ET03	10	2	9	1	21	8
SW0148	ET04	11	2	12	1	5	8
SW0159	ET06	13	2	16	1	1	8
SW0150	ET08	8	2	10	1	n.d.	n.d.
SW0152	ET07	11	2	10	1	12	8

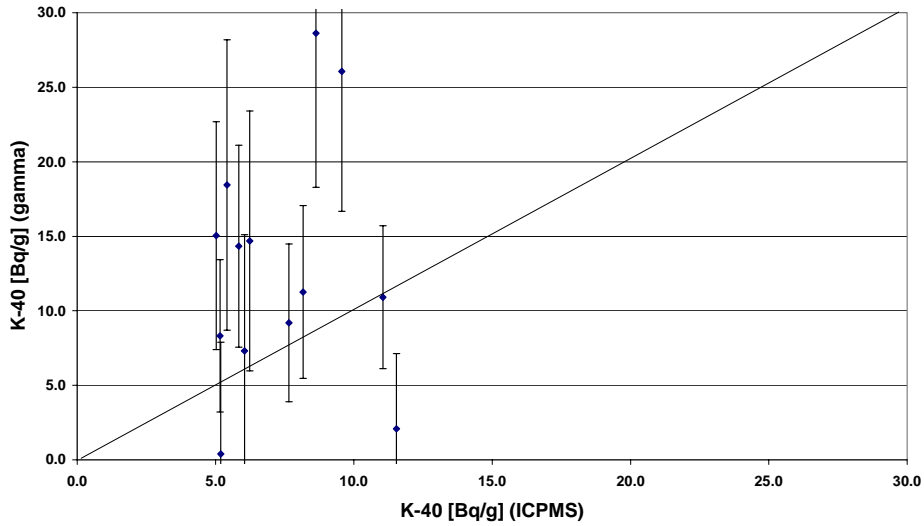


**Figure 5** Comparison of  $^{40}\text{K}$  data measured via gamma spectrometry at eriss and ICPMS and NTU. Uncertainties in  $^{40}\text{K}$ -activities are one standard deviation of counting statistics.

### 3.3 Chemistry

#### 3.3.1 Heavy Metals

Table 4 summarizes the results of the ICP-MS measurements of heavy metals, K, Mg, Al, Fe, Mn, Ba, Pb and U and  $^{206}\text{Pb}$ ,  $^{207}\text{Pb}$  and  $^{208}\text{Pb}$  isotopes in sediments from the Ngarradj catchment. In addition, figures 6 and 7 show the results of the copper, zinc, manganese, aluminium, iron and magnesium concentration measurements. The results for K concentrations, measured by ICPMS, are shown as well.

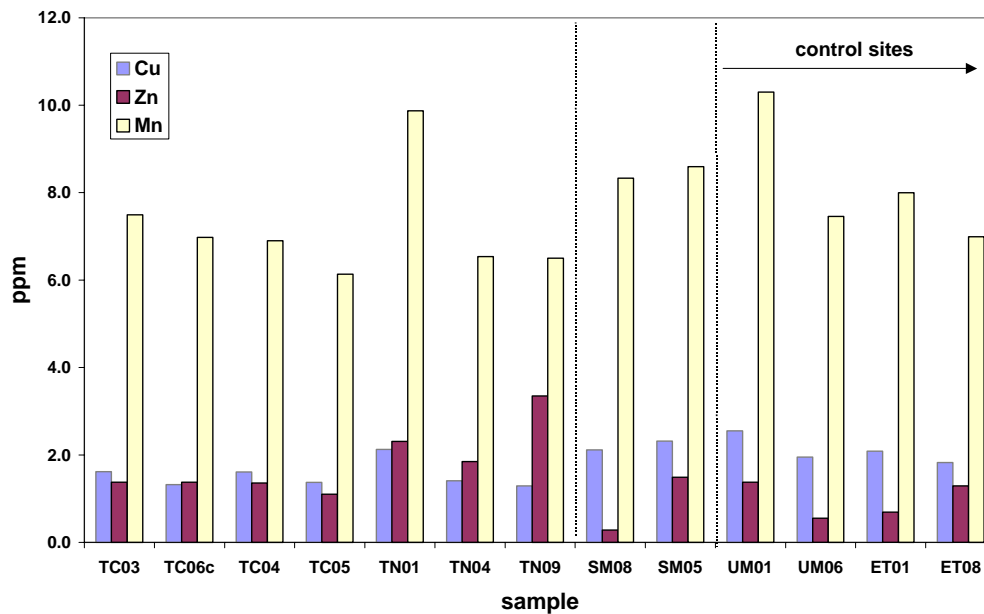


**Figure 6** Copper, zinc and manganese concentration measured by ICP-MS in sediments of the Ngarradj catchment

Sample	Mg	Al	K	Fe	Mn	Cu	Zn	Cd	Ba	U	Pb	$\frac{\text{Pb-208}}{\text{Pb-206}}$	$\frac{\text{Pb-207}}{\text{Pb-206}}$
<b>TC03</b>	77	4490	185	3070	7.492	1.621	1.380	0.027	3.573	0.363	1.200	1.896	0.633
<b>TC06c</b>	124	6030	303	3500	6.980	1.321	1.380	0.026	4.361	0.437	1.260	1.863	0.625
<b>TC04</b>	75	6170	159	3400	6.897	1.613	1.360	0.016	3.091	0.359	1.560	1.921	0.664
<b>TC05</b>	77	5420	171	2600	6.133	1.374	1.100	<0.010	2.969	0.349	1.420	1.892	0.643
<b>TN01</b>	164	11700	273	4900	9.872	2.128	2.310	0.016	7.702	0.675	2.200	1.946	0.662
<b>TN04</b>	96	5810	191	3540	6.537	1.411	1.850	<0.010	3.972	0.373	1.390	1.931	0.655
<b>TN09</b>	94	5400	163	2908	6.500	1.292	3.350	<0.010	4.350	0.368	1.492	1.931	0.664
<b>SM08</b>	41	1320	242	2190	8.333	2.117	0.280	<0.010	2.467	0.299	0.825	1.868	0.582
<b>SM05</b>	42	1450	258	2260	8.596	2.317	1.490	<0.010	2.601	0.296	1.100	1.888	0.638
<b>UM01</b>	44	1730	350	2600	10.300	2.551	1.380	0.038	3.006	0.326	0.954	1.853	0.595
<b>UM06</b>	45	1800	365	1905	7.457	1.954	0.553	0.029	2.862	0.301	0.878	1.838	0.582
<b>ET01</b>	49	1820	197	2360	7.996	2.088	0.691	<0.010	2.549	0.285	0.877	1.884	0.593
<b>ET08</b>	39	1608	164	2067	6.992	1.825	1.292	<0.010	2.242	0.298	0.950	1.853	0.610
<b>TC05-02</b>	45	3580	126	3690	1.487	0.307	0.646	<0.010	1.813	0.209	1.210	1.978	0.692
<b>TN01-02</b>	194	14300	304	6250	6.368	1.171	2.056	<0.010	10.600	0.688	2.410	1.966	0.678
<b>SM08-02</b>	37	1480	210	654	1.008	0.240	0.350	<0.010	1.964	0.074	0.652	2.056	0.682
<b>ET08-02</b>	22	1140	119	301	0.267	0.154	0.164	<0.010	1.389	0.054	0.530	2.075	0.674

**Table 4** ICP-MS results for heavy metals, Mg, K, U and Pb in ppm and Pb isotope ratios.

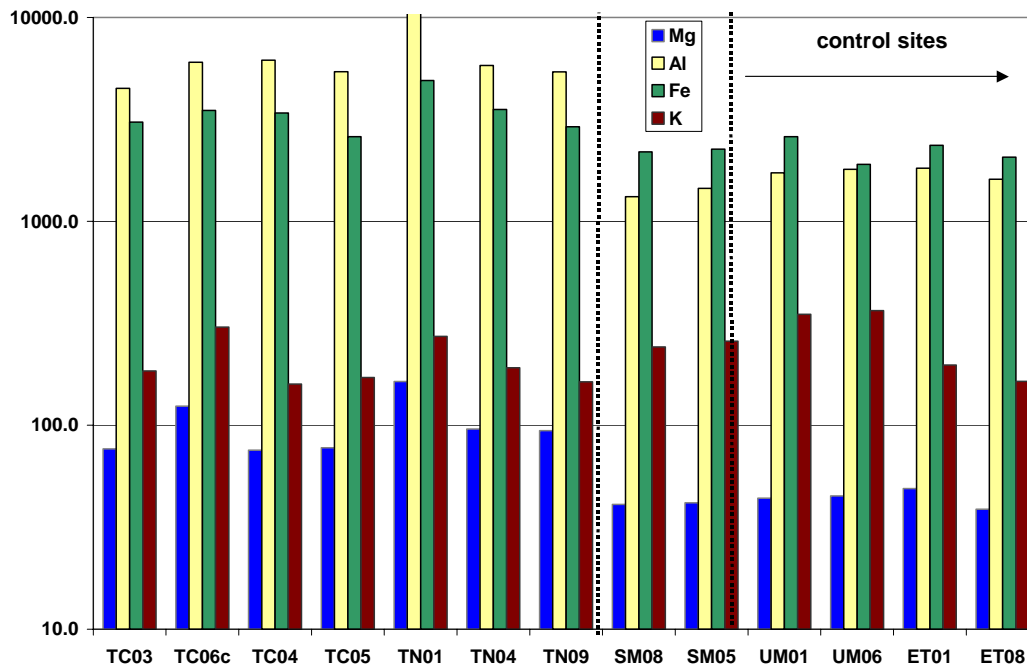


**Figure 7** Magnesium, aluminium, iron and potassium concentration measured by ICP-MS in sediments of the Ngarradj catchment. Note the logarithmic scale of the plot

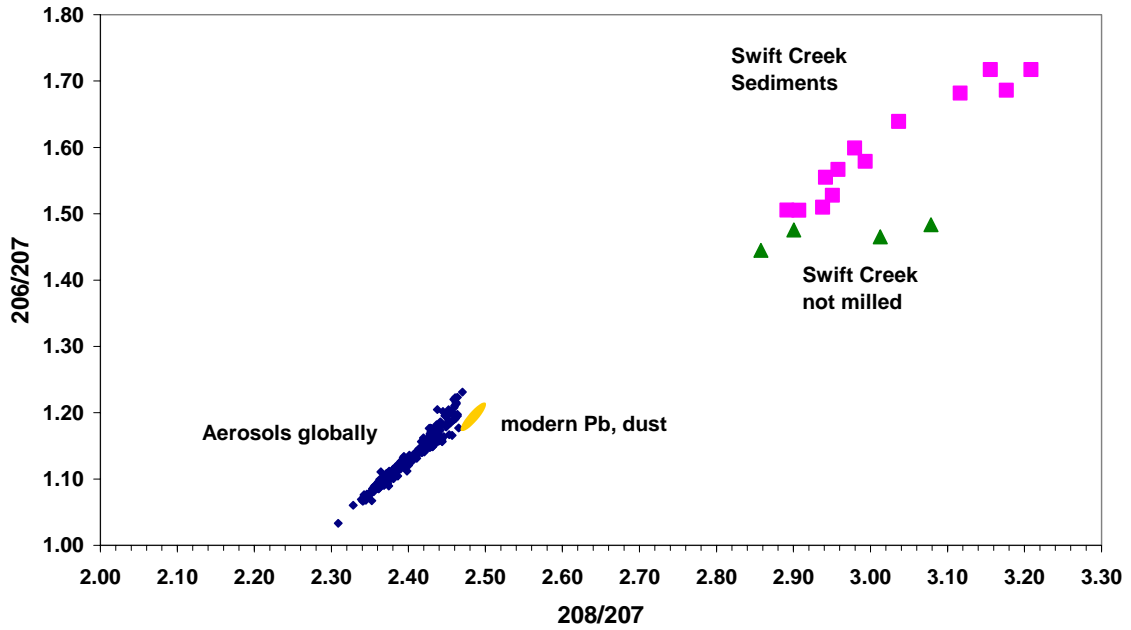
Whereas there appears to be no obvious trend in copper, zinc and manganese concentrations in the sediment samples (figure 6), figure 7 shows that the concentrations of the major elements aluminium, iron and magnesium are comparatively higher in Tributaries North and Central. This is most likely an effect of the higher clay content of the sandy sediments in those two tributaries (Saynor, pers. comm.).

### 3.3.2 Pb and Ra isotopes

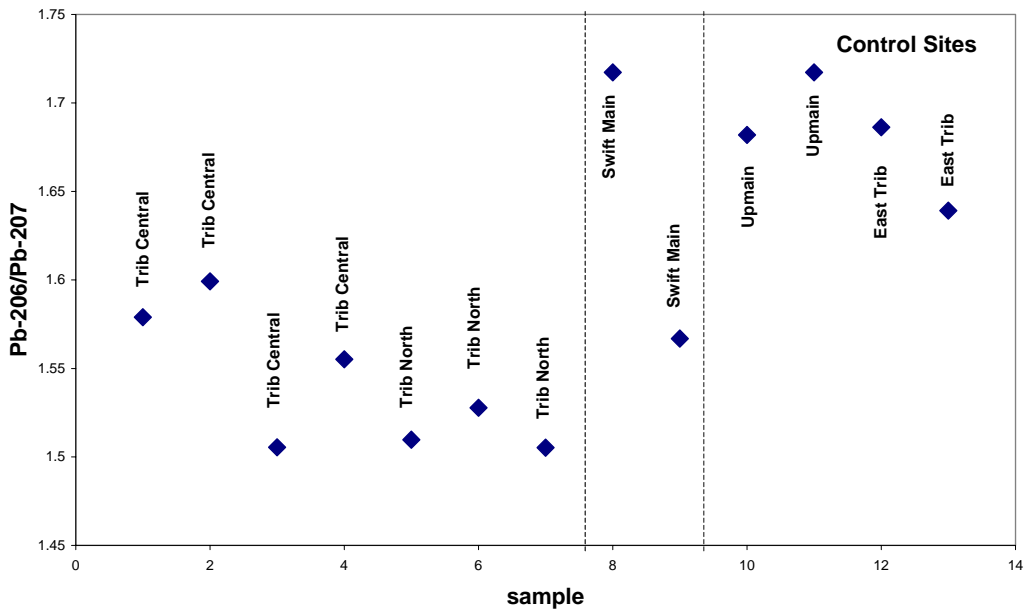
For means of easier comparison Pb isotope ratios measured in Ngarradj sediments are plotted as  $^{206}\text{Pb}/^{207}\text{Pb}$  versus  $^{208}\text{Pb}/^{207}\text{Pb}$  ratios. A contribution from the decay of U-rich materials to common Pb in the sample will be reflected in the three isotope plot by comparatively high  $^{206}\text{Pb}/^{207}\text{Pb}$  and low  $^{208}\text{Pb}/^{207}\text{Pb}$  isotope ratios (for example, Gulson et al., 1984, report  $^{206}\text{Pb}/^{207}\text{Pb}$  isotope ratios of up to 10 and  $^{208}\text{Pb}/^{207}\text{Pb}$  ratios as low as 0.05 in tailings) whereas Th-rich material will show up in the plots with comparatively high  $^{208}\text{Pb}/^{207}\text{Pb}$  isotope ratios.

Figure 8 shows the  $^{206}\text{Pb}/^{207}\text{Pb}$  plotted versus the  $^{208}\text{Pb}/^{207}\text{Pb}$  ratios measured in Ngarradj sediments and a comparison with typical common Pb isotope ratios and ratios measured in aerosols worldwide (Bollhöfer and Rosman, 2000,2001).  $^{206}\text{Pb}/^{207}\text{Pb}$  and  $^{208}\text{Pb}/^{207}\text{Pb}$  isotope ratios measured in the sediments indicate a significant contribution of radiogenic Pb to total Pb in sediments from the Ngarradj catchment. Assuming a common  $^{206}\text{Pb}/^{207}\text{Pb}$  isotope ratio of about unity and radiogenic  $^{206}\text{Pb}/^{207}\text{Pb}$  ratios, which typically range from 4 –15 and are produced by the concurrent decay of  $^{238}\text{U}$  and  $^{235}\text{U}$  (Doe, 1970), the contribution of radiogenic lead to common Pb is 5 – 25 per cent .

Both  $^{206}\text{Pb}/^{207}\text{Pb}$  and  $^{208}\text{Pb}/^{207}\text{Pb}$  isotope ratios are comparatively high, i.e. a relatively large amount of total Pb was produced from the decay of U and Th. In addition, whereas the  $^{206}\text{Pb}/^{207}\text{Pb}$  is different from the ratio expected in common Pb (Doe, 1970),  $^{208}\text{Pb}/^{206}\text{Pb}$  ratios are not far off 2.0 – 2.2 (see table 4), indicating that the U/Th ratio of the source of radiogenic Pb is similar to the U/Th ratio of the source of the common Pb.



**Figure 8** Pb isotope ratios of Ngarradj sediments in comparison with isotope ratios measured in aerosols worldwide (Bollhoefer and Rosman, 2001). Dust (Doe, 1970) and modern Pb (Munksgaard and Parry, 2000) are indicated on the plot as a yellow ellipse.



**Figure 9**  $^{206}\text{Pb}/^{207}\text{Pb}$  isotope ratios in sediments from Ngarradj. Pb isotope ratios are higher, i.e. more radiogenic for sediments from the control sites.

Pb isotope ratios in the sediment samples exhibit a grouping in their  $^{206}\text{Pb}/^{207}\text{Pb}$  (figure 9) and  $^{208}\text{Pb}/^{207}\text{Pb}$  ratios (figure 10). Whereas Pb isotope ratios are less radiogenic for samples from Tributaries North and Central, samples from the control sites along Tributary East, Upmain and the main channel of Ngarradj are more radiogenic with  $^{206}\text{Pb}/^{207}\text{Pb}$  ( $^{208}\text{Pb}/^{207}\text{Pb}$ ) isotope ratios as high as 1.715 (3.18).

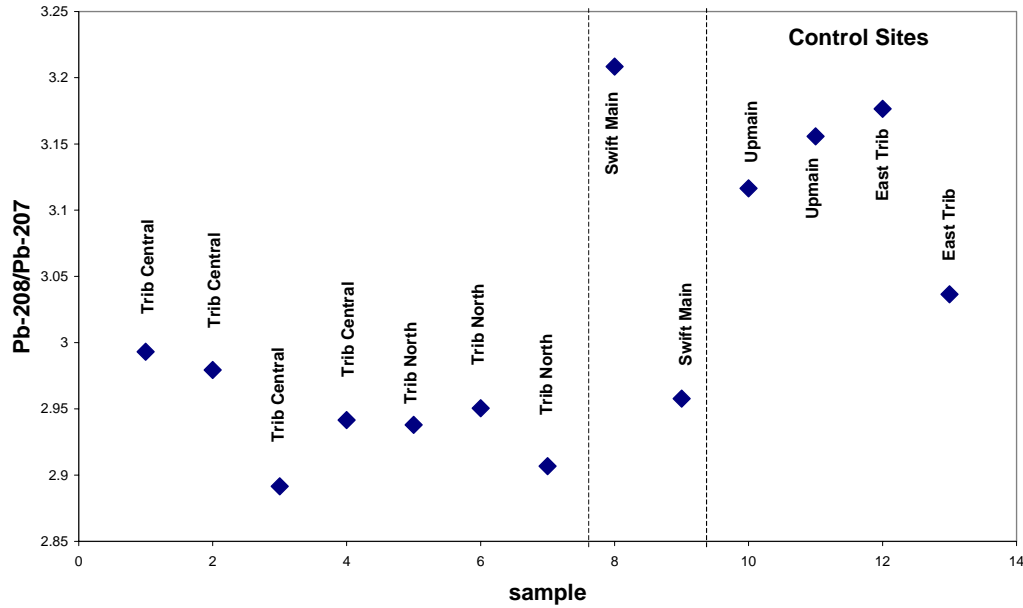


**Figure 10**  $^{208}\text{Pb}/^{207}\text{Pb}$  isotope ratios in sediments from Ngarradj. Pb isotope ratios are higher, i.e. more radiogenic for sediments from the control sites.

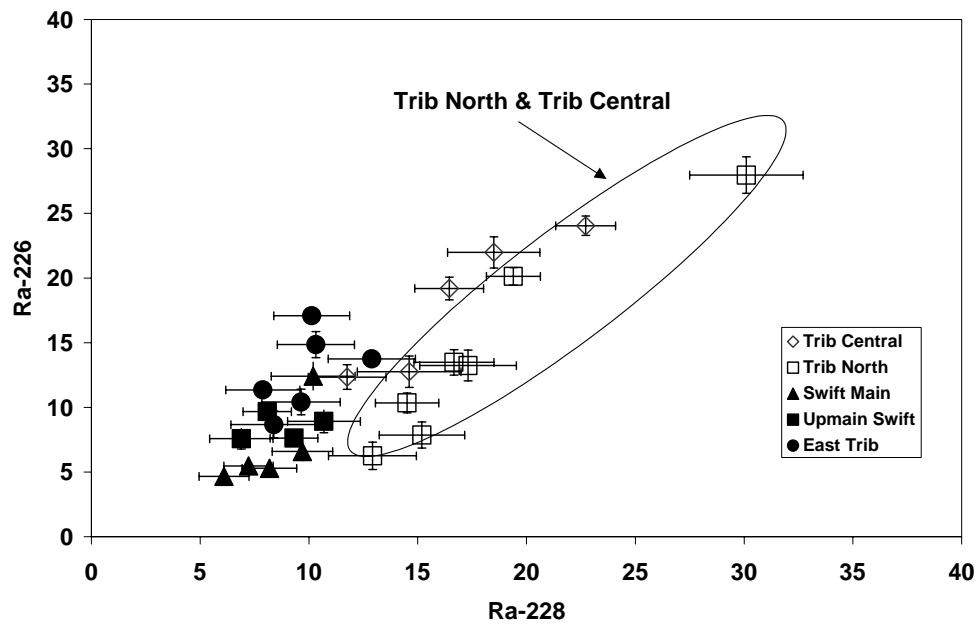


**Figure 11**  $^{226}\text{Ra}$  versus  $^{228}\text{Ra}$  activity concentration. Uncertainties are one standard deviation of counting statistics.

Although  $^{226}\text{Ra}$  and  $^{228}\text{Ra}$  activity concentrations are on average higher in sediment samples from Tributaries North and Central (figure 11),  $^{226}\text{Ra}/^{228}\text{Ra}$  isotope ratios do not exhibit an obvious difference between monitor and control sites (figure 12). This indicates that concentration variations observed are more likely to be natural and not influenced by erosion of uranium-mineralized material from the Jabiluka mine site, as this would create higher  $^{226}\text{Ra}/^{228}\text{Ra}$  isotope ratios in Tributaries North and Central. Moreover, the intercept with the y-axis in an inverse Ra concentration plot (figure 13) indicates that the source adding  $^{226}\text{Ra}$  to

the sediments within the Ngarradj catchment is relatively more enriched in  $^{226}\text{Ra}$ , a member of the U decay chain, at the control sites than it is at Tributaries North and Central. This further supports the conclusion that variations in Ra isotope concentrations observed in the sediments are not influenced by erosion of uranium-mineralized material.

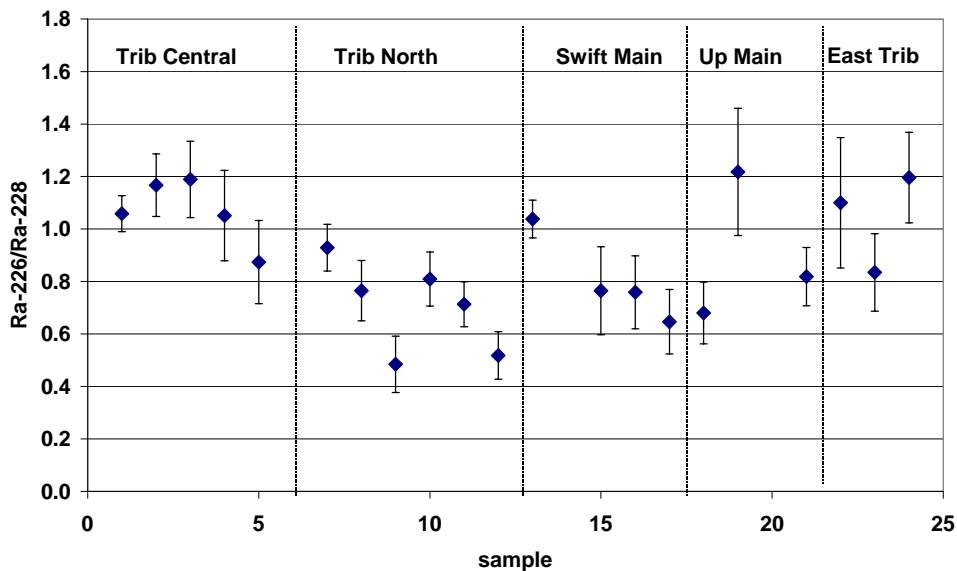


**Figure 12** Ra isotope ratios in the different tributaries in the Ngarradj catchment. Uncertainties are one standard deviation of counting statistics.

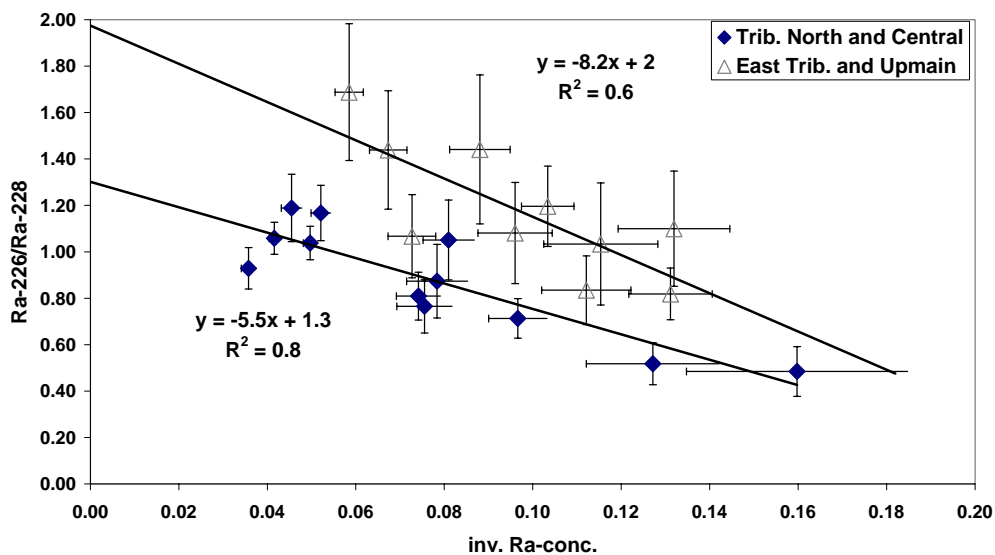


**Figure 13** Inverse  $^{226}\text{Ra}$  concentration plot. Uncertainties are one standard deviation of counting statistics.

## 4 Discussion

### 4.1 Characterization of Ngarradj sediments in comparison to other sediments within the Alligator Rivers Region

There are various studies focussing on sediments in the Alligator Rivers Region. For example, Clark et al. (1992) investigated sediments of the Magela floodplain in order to constrain sediment transport and deposition. They report U activity concentrations of 70 –90 Bq per kg across the floodplain, and  $^{232}\text{Th}$  and  $^{40}\text{K}$  activity concentrations of 73 – 104 Bq per kg and 156 –221 Bq per kg, respectively. Winde (2002) reports 50 – 100 Bq U per kg in sediments of Magela Creek, downstream of the Ranger mine, in accordance with sediments from the Magela floodplain. Magela Creek sands show very low  $^{238}\text{U}$ ,  $^{232}\text{Th}$  and  $^{40}\text{K}$  activity concentrations of approximately 15, 12 and 5 Bq per kg, respectively (Annual Research Summary, 1984-85). Other creeks in the Alligator Rivers region, for example sediments from the Goomadeer crossing in Arnhem Land show activity concentrations of 20, 16 and 100 Bq per kg (Ryan, unp. data).

**Table 5** Averages (or ranges) of  $^{238}\text{U}$ ,  $^{232}\text{Th}$  and  $^{40}\text{K}$  activity concentrations in sediments of the Alligator Rivers Region (Clark et al., 1992; Annual Research Summary, 1985; Winde, 2002; Ryan, unpublished data).

	Magela floodplain	Magela Creek	South Alligator River	Goomadeer River	Ngarradj catchment
$^{238}\text{U}$ [Bq/kg]	70 – 90	15	20 - 40	20	17
$^{232}\text{Th}$ [Bq/kg]	73 – 104	12	N/A	16	13
$^{40}\text{K}$ [Bq/kg]	156 –221	5	N/A	100	9

On average, Ngarradj sediments and its tributaries show U activity concentrations of approximately 17 Bq per kg (as calculated from gamma spectrometry results), an average of 13 Bq per kg for  $^{232}\text{Th}$  and 9 Bq per kg  $^{40}\text{K}$ , respectively. Within two standard deviations,  $^{226}\text{Ra}$  activity concentrations are in secular equilibrium with  $^{238}\text{U}$  in the sediment, however there is an excess of  $^{210}\text{Pb}$  in some of the samples. This excess in  $^{210}\text{Pb}$  results from the decay of  $^{222}\text{Rn}$  to  $^{210}\text{Pb}$  in the atmosphere and the subsequent deposition of  $^{210}\text{Pb}$  on the earth's surface.

Global averages for the U activity concentration in soils is about 1 ppm (Thornton, 1983), or approximately 12 Bq per kg. Stream sediments show quite large variations, dependent on their origin, but are usually higher than 1 ppm. For instance, stream sediments originating from weathering of granite complexes in Scotland show U concentrations of 2 – 10 ppm (Thornton, 1983). Our measurements show that U and Ra concentrations in Ngarradj sediments are similar to the global average and comparable with activity concentrations in sands from other creeks in the Alligator Rivers Region.

Compared with Magela floodplain or Goomadeer crossing sediments and the global average of approximately 250 Bq per kg (Thornton, 1983), potassium concentrations in Ngarradj catchment sediments are quite low. This may partly be due to the impact of saline waters at Magela floodplain and Goomadeer River and the fact that potassium is washed out of the Ngarradj sediments by fresh water during the wet season. Potassium concentrations are

comparable with concentrations in Magela Creek sands and there are no significant differences between control sites and Tributaries North and Central.

## 4.2 Radiogenic and Radioactive Isotopes

To our knowledge, until this study there were no data available on Pb isotope ratios of sediments within the Alligator Rivers region. Ngarradj sediment Pb isotope ratios are quite unusual, showing radiogenic  $^{208}\text{Pb}/^{207}\text{Pb}$  and  $^{206}\text{Pb}/^{207}\text{Pb}$  ratios.

Proterozoic (2500-543 Ma) granitic rock, migmatite schists and quartzite are major constituents of the Jabiluka area, and at areas adjacent to the main streams the basement rock is covered with sands (NT Government, Jabiluka Project ERA). The grab samples taken in October 2001 mainly consisted of sand, and the clay/silt content was consistently less than 10 per cent.

The anomalous Pb isotope ratios observed in the Jabiluka sands might be explained by the presence of U and Th rich minerals within the samples. Plotting the  $^{208}\text{Pb}/^{206}\text{Pb}$  ratios versus the Th concentration reveals a linear correlation with an R-squared of 0.7 (figure 14). This implies that the relatively higher  $^{208}\text{Pb}$  abundance in some of the samples is caused by the presence of Th rich material. Hence Th-rich minerals, such as monazites or ilmenite, originating from the weathering of granitic rocks in the Jabiluka area, may be responsible for the anomalous Pb isotope ratios observed.

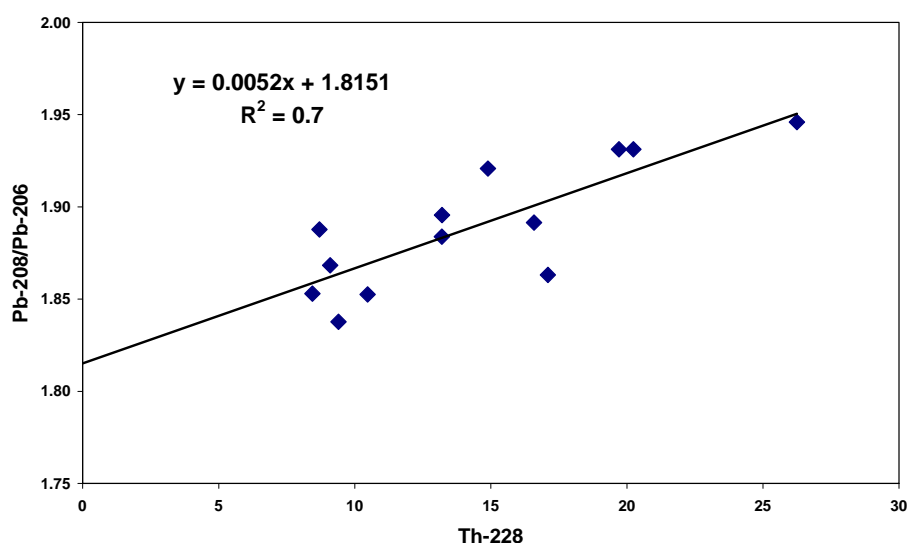


**Figure 14**  $^{208}\text{Pb}/^{206}\text{Pb}$  isotope ratios plotted versus thorium activity concentration

Munksgaard and Parry (2000, 2001) and Munksgaard et al. (1998) have investigated sediments in coastal and estuarine zones in northern Australia. In addition, there are studies investigating the fallout of mining derived particulates in northern Australia (Munksgaard and Parry, 1998) and particulates in tailings dam water (Gulson et al., 1992) of the ERA Ranger uranium mine. Munksgaard and Parry (2000) found anomalous lead isotope ratios, similar to but less radiogenic than our results, in offshore sediments in the Gulf of Carpentaria. They attribute the anomalous ratios to mixing of clay/silt with modern Pb isotope ratios with detrital monazite, originating from the weathering of granitic rock from the Georgetown Inlier of mainly Proterozoic age.

Furthermore, more radiogenic Pb isotope ratios in the samples from the East Tributary and Upmain Swift exhibit lower Al and Fe concentrations. This supports the assumption that Pb isotope ratios measured in the sediments reflect the mixing of detrital sands having relatively elevated Th contents and radiogenic Pb isotope ratios with clay and silt with higher Al and Fe concentrations but common Pb isotope ratios.

Such a mixing, similar to what was observed by Munksgaard and Parry (2000), is reflected in the three-isotope plot (figure 8), with Pb isotopic compositions of samples from Tributaries North and Central being located between modern Pb and East Tributary/Upmain Swift Pb isotope ratios. Hence, the relative proportion of clays and silt is higher in samples from Tributaries North and Central. The anomalous lead isotope ratios in offshore sediments in the Gulf of Carpentaria reported by Munksgaard and Parry (2000) would be located in between Ngarradj and modern Pb isotope ratios in figure 8.

Higher levels of clays and silts in Tributaries North and Central may reflect enhanced erosion from the Jabiluka mine site. However, it is unlikely that it is erosion from uranium-mineralized material such as ore, as the inverse Ra concentration plot (figure 13) indicates that the  $^{226}\text{Ra}/^{228}\text{Ra}$  ratios of the 'contaminating' end-member is comparatively low, lower than the Ra isotope ratios observed at the control sites.

Furthermore, plots of the Pb isotopic ratios versus the inverse Pb concentration (figure 15) support the scenario that the amount of natural clay and silt determines the concentration of Pb (and also Al, Fe and Mg) within sediments of the Ngarradj catchment. Inverse concentration plots are able to distinguish sources of 'contaminating' Pb and background Pb only if the background concentration is reasonably stable. This seems to be the case and end member  $^{206}\text{Pb}/^{207}\text{Pb}$ ,  $^{208}\text{Pb}/^{206}\text{Pb}$  and  $^{208}\text{Pb}/^{207}\text{Pb}$  isotopic ratios are  $1.32\pm 0.07$ ,  $2.00\pm 0.05$  and  $2.65\pm 0.12$  (95% confidence), respectively. This is close to the composition of modern crustal Pb, in dust, natural clays, silts and marine sediments (Doe, 1970).

We therefore assume that relatively radiogenic sands including heavy minerals, possibly monazites originating from the erosion of granites or granitic gneisses with comparatively low Pb concentrations, are mixed with natural dust, clays and silts, that contribute the majority of the Pb within the sediment. The contribution of Pb in monazites to the total Pb within the samples may be very small; however, due to their anomalous isotope ratios the small contribution will cause a drastic shift towards higher radiogenic Pb isotope ratios.

U rich material associated with uranium mining is characterized by very high  $^{206}\text{Pb}/^{207}\text{Pb}$  but low  $^{208}\text{Pb}/^{207}\text{Pb}$  ratios (see for example Gulson et al., 1992). There is no indication that there are erosion products from such material contaminating the sediments of the Ngarradj catchment. Additionally, Ra isotopes indicate that the relative contribution of U to the sediments appears to be higher for the control sites.

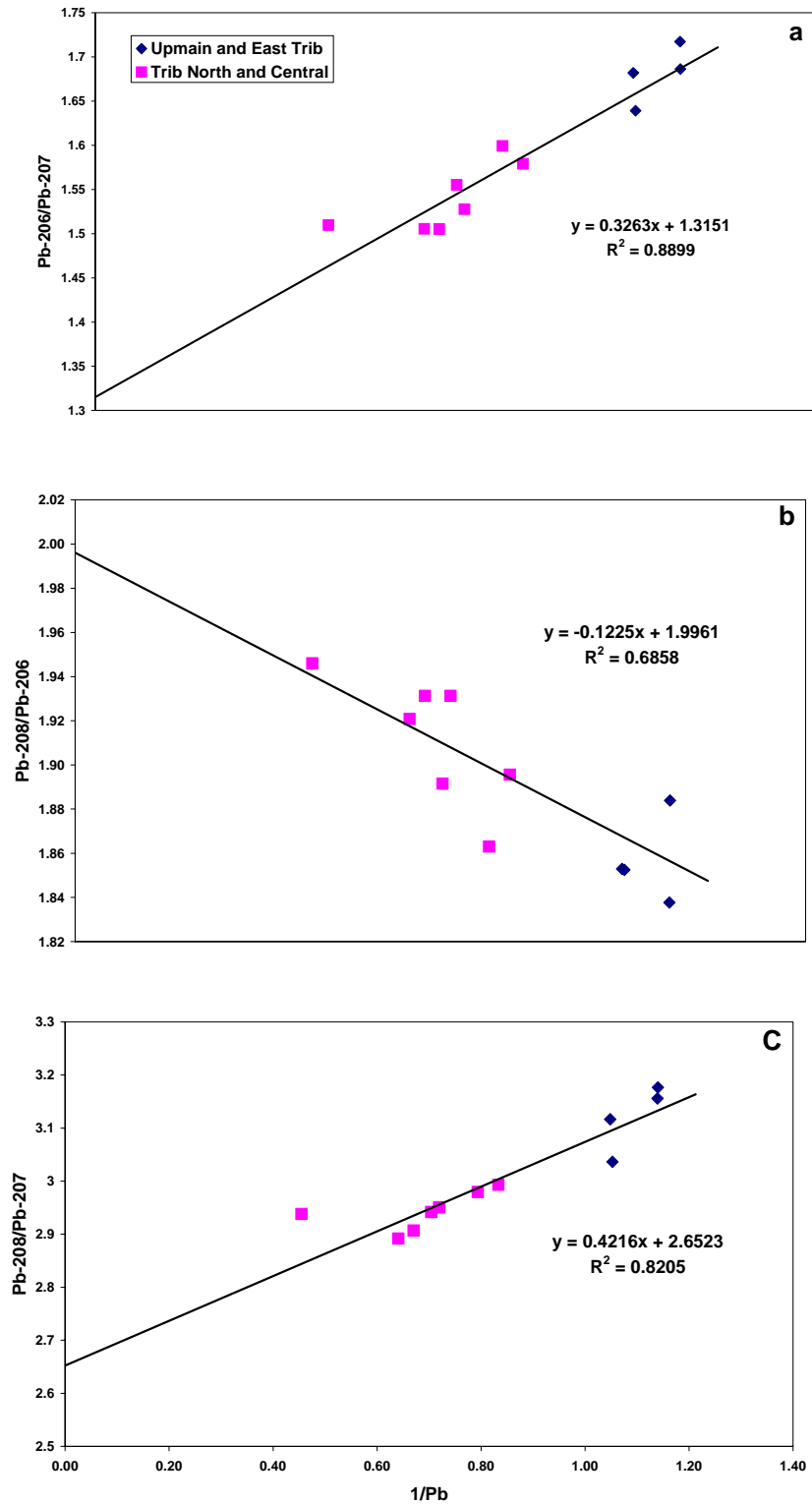


**Figure 15** Inverse Pb concentration plots identifying the source of contaminant Pb. End member  $^{206}\text{Pb}/^{207}\text{Pb}$  (a),  $^{208}\text{Pb}/^{206}\text{Pb}$  (b) and  $^{208}\text{Pb}/^{207}\text{Pb}$  (c) composition are  $1.32 \pm 0.07$ ,  $2.00 \pm 0.05$  and  $2.65 \pm 0.12$  (95% confidence), respectively.

Hence we conclude that present day variations in radiogenic and radioactive isotopes and heavy metals within sediments of the Ngarradj catchment are either natural, or that any contribution which may have arisen from erosion due to operations at Jabiluka has arisen from material without a significant U mineralization component.

## Acknowledgements

We thank the Hydrological and Ecological Processes section of *eriss*, in particular Bryan Smith, for the collection of samples in the Ngarradj catchment and Therese Fox for the sample preparation. In addition, gratefully acknowledged is Niels Munksgaard from the Northern Territory University for ICP-MS analysis and discussion of the results.

## References

- Alligator Rivers Region Research Institute, Annual Research Summary, 1984–85. Supervising Scientist, Canberra.
- Bollhöfer A & Rosman KJR 2000. Isotopic source signatures for atmospheric lead: The Southern Hemisphere. *Geochimica et Cosmochimica* 64, 3251–3262.
- Bollhöfer A & Rosman KJR 2001. Isotopic source signatures for atmospheric lead: The Northern Hemisphere. *Geochimica et Cosmochimica* 65, 1727–1740.
- Chiew FHS & Wang QJ 1999. *Hydrological analysis relevant to surface water storage at Jabiluka*. Supervising Scientist Report 142, Supervising Scientist, Canberra.
- Chow TJ, Snyder CB & Earl JL 1975. *United Nations FAO and International Atomic Energy Association Symposium*, Vienna, Austria (IAEA-SM-191/4), proceedings, pp 95–108.
- Clark RL, East TJ, Guppy J, Johnston A, Leaney F, McBride P and Wasson RJ 1992. Late Quaternary stratigraphy of the Magela Plain. In *Modern sedimentation and Late Quaternary evolution of the Magela Creek plain*, ed RJ Wasson, Research Report 6, Supervising Scientist, Canberra.
- Doe BR 1970, *Lead Isotopes*, Springer-Verlag Berlin, Germany.
- Gulson BL, Mizon KJ, Korsch MJ, Carr GR, Eames J & Akber RA 1992, Lead isotope results for waters and particulates as seepage indicators around the Ranger uranium tailings dam – a comparison with the 1984 results. Open File Report 95, Supervising Scientist, Canberra.
- Johnston A & Prendergast JB 1999. *Assessment of the Jabiluka Project: Report of the Supervising Scientist to the World Heritage Committee*. Supervising Scientist Report 138, Supervising Scientist, Canberra.
- Marten R 1992. Procedures for routine analysis of naturally occurring radionuclides in environmental samples by gamma-ray spectrometry with HPGe detectors. Internal report 76, Supervising Scientist for the Alligator Rivers Region, Canberra. Unpublished paper.
- Munksgaard NC & Parry DL 2000. Anomalous lead isotope ratios and provenance of offshore sediments, Gulf of Carpentaria, Australia. *Australian Journal of Earth Sciences* 47, 771–777.
- Munksgaard NC & Parry DL 2001. Trace metals, arsenic and lead isotopes in dissolved and particulate phases of North Australian coastal and estuarine seawater. *Marine Chemistry* 75, 165–184.
- Munksgaard NC, Batterham GJ & Parry DL 1998. Lead isotope ratios determined by ICP-MS: Investigation of anthropogenic lead in Seawater and sediment from the Gulf of Carpentaria, Australia. *Marine Pollution Bulletin* 36(7), 527–534.

- Northern Territory Government Department of Lands, Planning and Environment 1997. *Assessment Report 22, Jabiluka number 2 uranium mine proposal, Environmental Assessment Report and Recommendations by the Environment Protection Division*, August 1997.
- Rosman KJR, Chisholm W, Boutron CF, Candelone JP, Görlach U 1993. Isotopic evidence for the source of lead in Greenland snows since the late 1960s. *Nature* 362, 333–334.
- Rosman KJR, Chisholm W, Hong S, Candelone J & Boutron CF 1997. Lead from Carthaginian and Roman Spanish mines Isotopically Identified from 600BC to 300AD. *Environmental Science and Technology* 31, 3413–3416.
- Thornton I (ed) 1983. *Applied Environmental Geochemistry*. Academic Press Geology Services.
- Winde F 2002. Stream pollution by adjacent tailing deposits and fluvial transport of dissolved uranium – dynamics and mechanisms investigated in mining areas of Germany, Southern Africa and Australia. In *Uranium in the aquatic environment*, eds Merkel BJ, Planer Friedrich B & Wolkersdorfer C, Springer-Verlag, Berlin, Heidelberg, New York.